Dynamical bimodality in equilibrium monostable systems

M. Mierzejewski, J. Dajka, and J. Łuczka
Institute of Physics, University of Silesia, 40-007 Katowice, Poland

P. Talkner and P. Hänggi
Institute of Physics, University of Augsburg, Universitätsstr. 1, D-86135 Augsburg, Germany

(Received 4 July 2006; published 2 October 2006)

General features of the stochastic dynamics of classical systems approaching a thermodynamic equilibrium Gibbs state are studied via the numerical analysis of time-dependent solutions of the Fokker-Planck equation for an overdamped particle in various monostable potentials. A large class of initial states can dynamically bifurcate during its time evolution into bimodal transient states, which in turn wear off when approaching the long-time regime. Suitable quantifiers characterizing this transient dynamical bimodality, such as its lifetime, the positions of maxima, and the time-dependent well depth of the probability distribution, are analyzed. Some potential applications are pointed out that make use of this interesting principle which is based on an appropriately chosen initial preparation procedure.

DOI: 10.1103/PhysRevE.74.041102 PACS number(s): 05.20.−y, 05.70.Ln, 05.40.−a

I. INTRODUCTION

Multistable systems frequently occur in nature and therefore are of eminent importance for various disciplines of science. Closely related to the phenomenon of multistability are problems such as the stability of states, activation processes, phase transitions, exit times of locally stable states, escape over energy barriers, etc. [1,2]. Bistable systems provide the simplest but yet nontrivial and important case of multistable systems. Examples of such systems can be found in physics, chemistry, and biology [1–4]. They typically describe quite different physical systems in regard to their explicit dynamics, nevertheless, these multistable systems exhibit a common universal behavior. This universality is fundamental. Often, bistability is a feature of steady states suddenly showing up upon a change of a control parameter. At a critical value of the control parameter the number of stable asymptotic states increases from one to two. Optical bistability [5,6] is just one of many examples illustrating such a bifurcation of steady states. Phase transitions provide a whole variety of other examples. We also note that asymptotic states that display a persistent dynamics such as stable limit cycle dynamics or chaotic attractors may coexist. Here all types of combinations between coexisting stationary metastable states and dynamic metastable states may occur.

The presence of noise in a deterministically bistable system tends to smear out the sharp deterministically localized states and to let the system explore larger regions of its state space. If the noise though is small enough, the system will stay most of the time in either of the two stable states, and only occasionally trigger a transition between these states. As a consequence, the probability density then displays a *bimodal* structure with pronounced maxima at the deterministic states. On the other hand, bimodality of a system's probability density does not necessarily imply its bistability. An initially prepared double humped probability density of a monostable system will survive for some time until it eventually disappears. Also the probability density of a system that linearly oscillates back and forth displays maxima at the two points of return. In this paper, we demonstrate that bimodality can result in a monostable system from an unimodal, i.e., one humped probability density as a transient effect.

The layout of the paper is as follows: In Sec. II, we formulate the problem in terms of a Brownian particle moving in a one-dimensional potential. Examples of specific models are presented in Sec. III. In Sec. IV we analyze in detail transient bimodality. Section V contains conclusions. In the Appendix, we derive an equation for the mean time of first exit, the behavior of which explains bimodality in monostable systems.

II. BROWNIAN PARTICLE IN A POTENTIAL

A broad class of systems in contact with a thermostat can be modeled by a one-dimensional Langevin equation describing the position x of an overdamped Brownian particle randomly moving in a potential $V(x)$ [1,7]. It reads in appropriate chosen dimensionless units,

$$\dot{x} = -V'(x) + \sqrt{2D}\Gamma(t), \tag{1}$$

where the dot denotes the derivative with respect to time t and the prime is the derivative with respect to the coordinate x of the Brownian particle. The random force $\Gamma(t)$ describes thermal noise. It is modeled by zero-mean Gaussian delta-correlated white noise of unit intensity, i.e., $\langle \Gamma(t)\Gamma(s)\rangle = \delta(t-s)$. The parameter $D=D(T)\propto T$ is proportional to temperature T of the thermostat. The Langevin equation (1) defines a Markov diffusion process. The corresponding probability density $p(x,t)$ obeys the Fokker-Planck equation [7,8]

$$\frac{\partial}{\partial t}p(x,t) = \frac{\partial}{\partial x}V'(x)p(x,t) + D\frac{\partial^2}{\partial x^2}p(x,t) \tag{2}$$

with an arbitrary initial condition $p(x,0)$. All potentials that we will consider here grow to infinity for $|x|\to\infty$. In these cases, natural boundary conditions apply, i.e., the probability density approaches zero outside of some central region, i.e., $p(x,t)\to 0$ as $|x|\to\infty$.

The stationary probability density $p_{st}(x)$ is then uniquely approached in the limit of long times; it assumes the form of

a Gibbs state describing thermal equilibrium at the thermostat temperature T, namely,

$$p_{st}(x) \propto \exp[-V(x)/D]. \tag{3}$$

For a potential having two minima and a maximum in between, the deterministic dynamics for the Brownian particle described by Eq. (1) is, in the limit $T \to 0$, bistable with the stable states located at the positions of the potential minima. Clearly, in the presence of noise, the corresponding stationary probability density becomes bimodal. Accordingly, a potential with a single minimum is monostable and the corresponding probability density is unimodal. In this paper we will describe a generic mechanism that produces a *dynamical bimodality* which evolves from a unimodal initial state. The time dependent probability density $p(x,t)$ can then be expressed in terms of a nonequilibrium potential $\Psi(x,t)$, reading

$$p(x,t) \propto \exp[-\Psi(x,t)], \tag{4}$$

which changes with time as a function of x from a single minimum to one possessing two minima, and finally approaches asymptotically its equilibrium form given by $V(x)/D$ exhibiting a single minimum.

III. MODEL SYSTEMS

We consider a reflection-symmetric potential $V(x)$ with a single minimum at $x=0$. Its leading contribution near the origin is parabolic with curvature $\epsilon > 0$. The potential can be presented as

$$V(x) = \frac{\epsilon}{2}x^2 + h(x), \tag{5}$$

where $h(x)$ describes the deviation from the harmonic potential with $h(0)=h'(0)=h''(0)=0$. Due to the symmetry of the potential its leading contribution for small values of x is proportional to x^4; i.e.,

$$h(x) = \alpha x^4 + \cdots \quad \text{for } |x| \ll 1, \tag{6}$$

where α denotes a positive constant.

There are several important physical examples for such symmetric, monostable potentials. Below, we present three of them, which will be discussed in greater detail with this work.

A. Ginzburg-Landau model

The first example is the celebrated zero-dimensional Ginzburg-Landau (GL) model [9,10] displaying a second-order phase transition. In this case, higher-order terms in Eq. (6) are neglected. The parameter ϵ measures the relative distance of temperature from its critical value T_c, i.e., $\epsilon \propto T/T_c - 1$. In the high-symmetry phase ($\epsilon \geqslant 0$), which will be considered here, the potential $V(x)$ is monostable; in contrast, when the spontaneous symmetry breaking takes place below T_c, the potential $V(x)$ assumes a bistable form.

B. Josephson junction

The second example presents the case of the resistively shunted junction model of a trapped magnetic flux y in a superconducting ring interrupted by a Josephson junction (JJ) [11]. In this case the potential reads

$$V(y) = \frac{1}{2}(y - \phi_{ext})^2 - E_0 \cos(2\pi y), \tag{7}$$

where ϕ_{ext} is the external magnetic flux and E_0 denotes the Josephson coupling energy which depends on the junction properties. In the following we consider only half integer values of ϕ_{ext} and introduce $x=y-\phi_{ext}$. The use of the parametrization

$$E_0 = (1-\epsilon)/4\pi^2 \tag{8}$$

transforms $V(y)$ in Eq. (7) to the form given by Eqs. (5) and (6), with

$$\alpha = \pi^2(1-\epsilon)/6. \tag{9}$$

It can readily be checked that $V(x)$ is monostable (bistable) for $\epsilon \geqslant 0$ ($\epsilon < 0$), in analogy to the case of the GL model.

C. Mesoscopic rings (MR)

The third physical situation addresses a model of noise assisted persistent currents in mesoscopic systems of cylindrical symmetry assuming the form of rings, cylinders, or tori [12,13]. The magnetic flux x dynamics is governed by a potential of the form

$$V(x) = \frac{1}{2}x^2 + I_0 \sum_{n=1}^{\infty} \frac{A_n(T)}{2\pi n} \times \{p\cos[2\pi n x] + (1-p)\cos[2\pi n(x+1/2)]\}, \tag{10}$$

where the prefactor I_0 is the maximal value of the persistent current at temperature $T=0$. It depends on the electronic and geometric properties of the system (e.g., on the circumference of the ring). The quantity $p \in [0,1]$ denotes the probability of a single channel with an even number of electrons within a multichannel ring. The harmonic weights $A_n(T)$ depend on temperature T via the ratio T/T^*, wherein T^* denotes the characteristic temperature determined from the relation $k_B T^* = \Delta_F/2\pi^2$ and Δ_F is the energy gap at the Fermi level. In this case, the dimensionless noise intensity $D=\delta_0 T/T^*$, where $\delta_0 = k_B T^*/2\epsilon_0$. The parameter ϵ_0 is the magnetic energy of the flux quantum. The explicit form of $A_n(T)$ is given, e.g., in Ref. [14]. Because of their dependence on temperature T, also the potential $V(x)$ depends explicitly on temperature T. Expanding the cosine functions into a Taylor series, one can show that for small x the potential corresponding to Eq. (10) takes the form (5) with the expansion coefficients ϵ and α expressed as infinite series in terms of the weighting factors $A_n(T)$. At high temperatures the potential is monostable and changes to a bistable potential upon lowering temperatures or by raising I_0.

On one hand, in the vicinity of $x \approx 0$, all the above examples take on a common form of the Ginzburg-Landau model, which is an archetypical model of critical behavior. On the other hand, both the JJ and MR models behave dif-

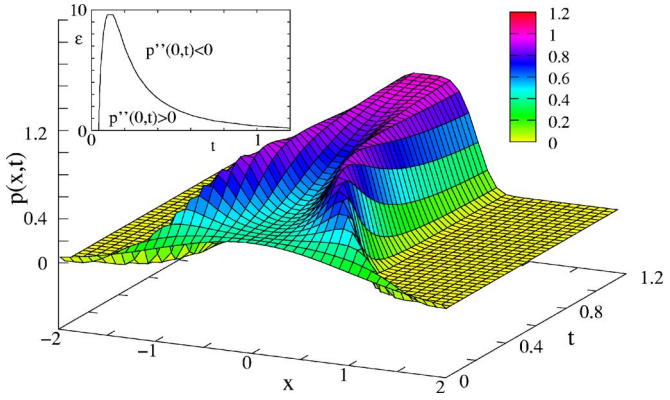

FIG. 1. (Color online) Time evolution of $p(x,t)$ in the Ginzburg-Landau model with $D=0.1$, $\epsilon=0$, and $\alpha=1$ from the initial Gaussian distribution $p(x,0)=1/\sqrt{2\pi}\exp(-x^2/2)$. The inset depicts the curve where the second-order spatial derivative of the probability density $p''(0,t)$ vanishes on the (ϵ,t) plane. Dynamical bimodality occurs below this curve where $p''(0,t)>0$.

ferently for large values of x compared to the GL model. In the case of the GL model, $V(x)$ depends on temperature and grows as x^4 for $|x|\to\infty$. In the case of the JJ model, $V(x)$ is temperature independent and $V(x)/x^2$ is bounded. The case of the MR is intermediate in the sense that $V(x)$ is temperature dependent and $V(x)/x^2$ remains finite for arbitrary large x. We systematically restrict the following discussion to the regime $(\epsilon \geqslant 0)$ only when the stationary state is monostable.

IV. DYNAMICAL BIMODALITY

We investigated the dynamics of the above-described systems by numerical solutions of the Fokker-Planck equations with the potentials (5)–(10) in the monostable regime with an initially unimodal symmetric probability density which is *broader* than the respective equilibrium distribution, i.e., its initial variance exceeds the equilibrium variance. In this case the time-dependent probability density evolves a bimodal character as a function of time and remains in this bimodal state for some time span τ_s until it eventually approaches its unique, unimodal equilibrium shape (3), see Fig. 1.

Our main goal is to characterize and understand this intriguing *transient* bimodality. To this end, we introduce various quantifiers of this phenomenon: (i) The positions $\pm x_M(t)$ of minima of the time-dependent potential $\Psi(x,t)$ in Eq. (4) representing the most probable values of the symmetric stochastic process $x(t)$ in Eq. (1), i.e., these positions correspond to maxima of the probability density $p(x,t)$ with the minimum of the bimodal probability being located at $x=0$; (ii) the barrier height $\Delta\Psi(t)=\Psi(x=0,t)-\Psi(x=x_M,t)$ of the potential and, directly related, the relative depth $d(t)=[p(x_M,t)/p(0,t)]-1$ of the well of the probability density; (iii) the lifetime $\tau_s=t_2-t_1$ of the bimodal state, which elapses from the onset of the bimodality at t_1 until its disappearance at t_2. The bimodality sets in when the probability density at $x=0$ changes from a maximum to a minimum and it disappears again when the minimum again turns into a maximum, i.e., $\partial^2 p(0,t_{1,2})/\partial x^2=0$ with $\partial^2 p(0,t)/\partial x^2>0$ for $t_1<t<t_2$. It can equivalently be characterized by the conditions $d(t)>0$ or $x_M(t)\neq 0$. The bimodality is more pronounced are the larger the values of the so introduced three quantifiers.

A. Lifetime of bimodality

In Figs. 2 and 3 we present the dependence of $x_M(t)$ and $d(t)$ on the criticality parameter ϵ for the three above mentioned systems, GL, JJ, and MR. As a function of evolution time t, the position of the maxima $x_M(t)$ and the relative depth $d(t)$ exhibit a bell-shaped form, i.e., they remain zero until a time t_1, then grow rapidly until they reach a maximum, and finally decrease until they vanish at t_2. The dynamical bimodality occurs for all three potentials, GL, JJ, and MR, and therefore this phenomenon happens to be quite independent of the asymptotic properties of $V(x)$ for large x. The bimodality becomes more pronounced for smaller values of ϵ, i.e., when the quartic contribution dominates over the

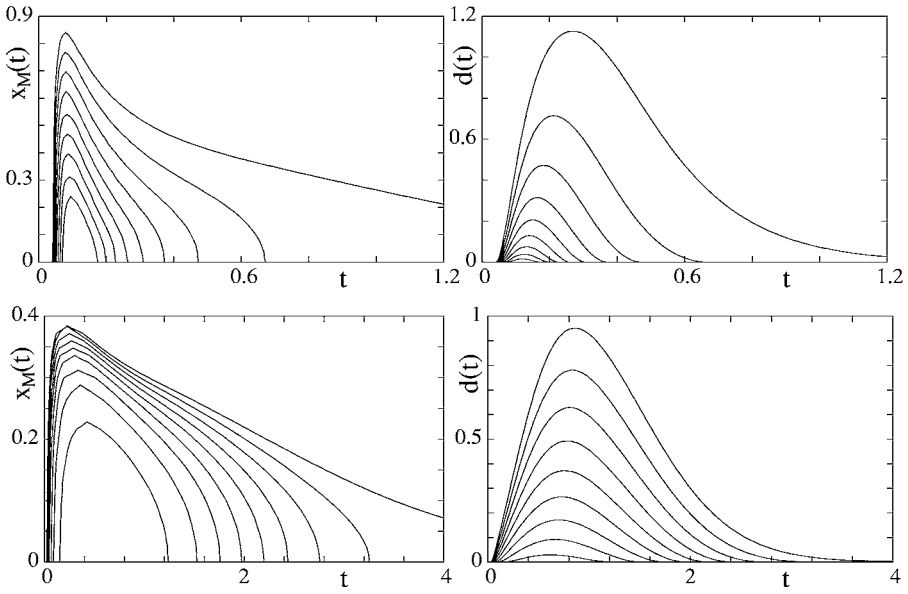

FIG. 2. Left panels: Time evolution of the most probable position $x_M(t)$. Right panels: Time evolution of the bimodality depth $d(t)$. The upper panels show results obtained for the Ginzburg-Landau model with $\alpha=1$. The curves from top to bottom correspond to $\epsilon=0,1,2,\ldots,8$, respectively, and the noise intensity $D=0.1$. The lower panels show results obtained for the Josephson-junction model. The curves from top to bottom correspond to $\epsilon=0,0.1,\ldots,0.8$ and $D=0.02$. In this case, the values of α are given by Eq. (9). The initial distribution is the same as in Fig. 1.

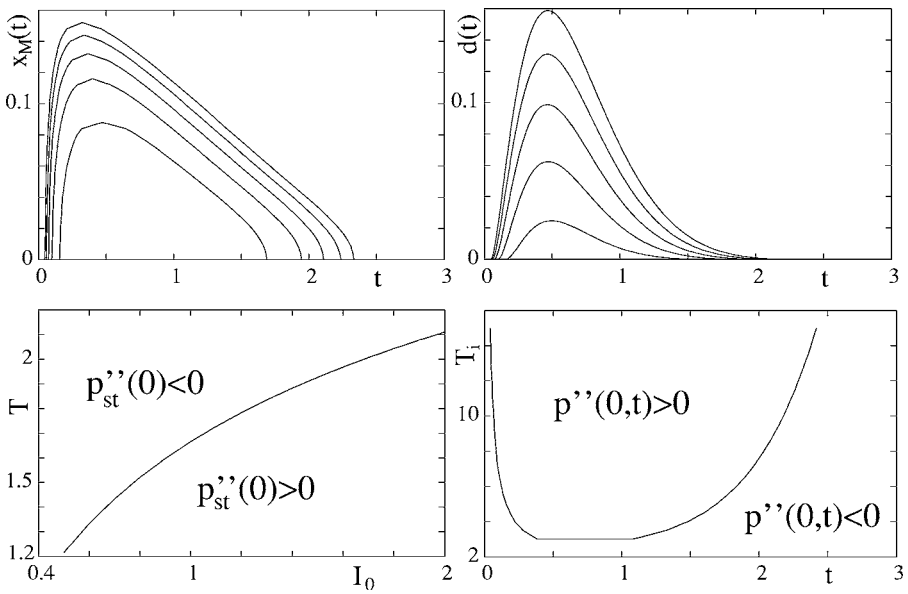

FIG. 3. Results for the mesoscopic rings with $I_0=1$ and $D=0.01T$. Upper panels: Time evolution of $x_M(t)$ (left) and the bimodality depth $d(t)$ (right). The system evolves from $p(x,0)=p_{st}(x)$ for the initial temperature $T=T_i$ to the final stationary state $p_{st}(x)$ with temperature $T=T_f=1.7$. The curves from bottom to top are obtained for the initial temperature $T_i=5$, 7, 9, 11, 13, respectively. Lower panels: Left panel shows the bistability diagram for the equilibrium state. The right panel shows the region in the (T_i,t) plane, where the dynamical bimodality occurs, $p''(0,t)>0$.

parabolic part of the potential already for rather small x value. It is remarkable that the lifetime τ_s increases with decreasing ϵ and diverges at the critical point $\epsilon=0$. On the other hand, if ϵ is too large, the bimodality does not occur at all. This is illustrated in the inset in Fig. 1, which presents a "phase diagram" in the (ϵ,t) plane. The solid line separates the regions where the second derivative $\partial^2 p(0,t)/\partial x^2$ of the probability density changes sign constituting the boundary between bimodal $[\partial^2 p(0,t)/\partial x^2>0]$ and unimodal $[\partial^2 p(0,t)/\partial x^2<0]$ probability densities. While the lifetime τ_s can vary from zero to infinity, the other two quantities $x_M(t)$ and $d(t)$ remain bounded for all evolution times t and parameter values. In particular, they converge to a finite value if $\epsilon\to 0$.

B. Role of initial states

The onset of the dynamical bimodality depends also on the choice of the initial distribution. As emphasized already above, the initial distribution $p(x,t=0)$ should be broader than the equilibrium distribution $p_{st}(x)$. If the initial state is Gaussian with the distribution $p(x,t=0)=\exp[-x^2/2\sigma^2]/\sqrt{2\pi\sigma^2}$, the bimodality occurs only if $p(x=0,t=0)/p_{st}(0)<1$, see Figs. 1 and 2. It is more pronounced for lower values of this ratio, i.e., for broader initial distributions with larger values of the variance σ^2. Another class of initial distributions is provided by thermal equilibrium states as in Eq. (3), but being prepared at higher temperatures. In the case of temperature-independent potentials, a broad initial distribution can be achieved by heating up the system to a sufficiently high temperature. Upon a sudden quenching [10], $p(x,t)$ evolves from a broader probability distribution to a narrower one (see the right panel of Fig. 4). For temperature-dependent potentials, the variance is not necessarily a monotonic function of temperature and the above statement may not hold true. However, we have found that also in this case the bimodality can be induced by sudden cooling provided that the ratio ϵ/α in the potentials (5) and (6) is small enough. Such a situation is depicted in Fig. 3 and in the left panel of Fig. 4.

C. Origin of bimodality

In order to unravel the mechanism that generates a bimodal from a unimodal probability density in a monostable sys-

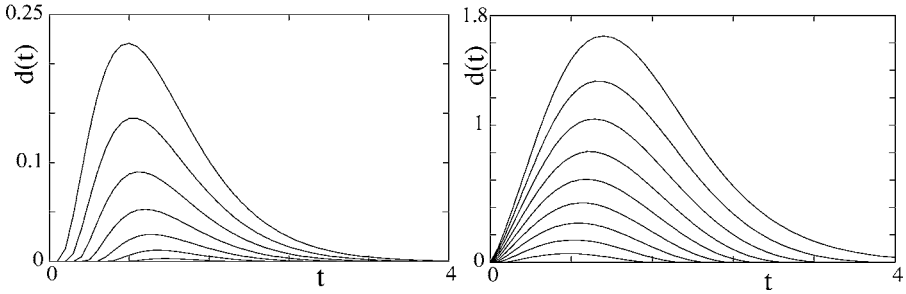

FIG. 4. Time evolution of the bimodality depth originating from a sudden drop of temperature. The system evolves from $p(x,0)=p_{st}(x)$ for the initial temperature $T=T_i$ to the final stationary state $p_{st}(x)$ with temperature $T=T_f$. Assumed value of $D=0.1T$. The left panel shows results obtained for the Ginzburg-Landau model with $T_i=10$, $T_f=1.3$, and $\alpha=0.1$. Here, the curves from top to bottom correspond to $\epsilon=\epsilon_0(T-1)$ with $\epsilon_0=0.02,0.04,\ldots,0.14$. The right panel shows results obtained for the Josephson junction model with $T_i=10$ and $T_f=0.1$. The curves from the top to the bottom correspond to $\epsilon=0,0.1,\ldots,0.8$.

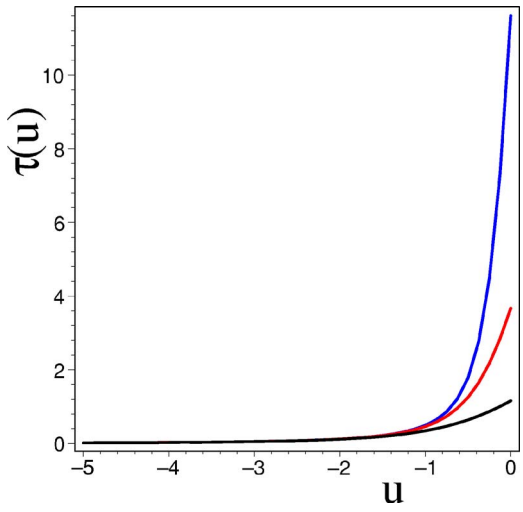

FIG. 5. (Color online) Mean first time (A2) to reach the point u from the starting point $x_0=-10$ for a particle governed by the Langevin equation (1) with the potential $V(x)=x^4/4$ and different noise intensity $D=1$, 0.1, 0.01 from bottom to top.

tem we consider a single random trajectory in the archetypical potential described by Eqs. (5) and (6). As an initial condition for the considered trajectory we choose a point that is remote from the origin. There, the large deterministic force resulting from the quartic part of the potential does dominate both the random and the linear contributions to the force. Consequently, the trajectory will display a fast and almost deterministic motion until a neighborhood of the origin is reached where either the linear or the random force dominates. From there on, the final approach to the origin is much slower than the initial deterministic motion. Therefore in an ensemble of particles, an accumulation of trajectories will result just in the region where the deterministic contribution of the quartic potential loses its dominance. This qualitative mechanical picture also allows to understand the dependence of the effect on the initial distribution: Only from a sufficiently broad distribution the fraction of remote particles is large enough in order to cause a "congested traffic situation."

A quantitative corroboration of this qualitative picture can be obtained by considering the time that it takes to reach a final destination $x=u$ for the first time from an initial point $x=x_0$. The mean value $\tau(u)=\mathcal{T}_{x_0}(x_0\to u)$ of this "first exit time" is the solution of the inhomogeneous backward equation:

$$\left[-V'(u)\frac{d}{du}+D\frac{d^2}{du^2}\right]\tau(u)=1 \tag{11}$$

with homogeneous "initial conditions" reading

$$\tau(x_0)=0, \quad \tau'(x_0)=0. \tag{12}$$

For a derivation of this equation we refer to the Appendix. In Fig. 5, we depict the mean time $\tau(u)=\tau(x_0\to u)$ as a function of the exit point u. For the remote starting point $x_0=-10$ the first exit time only slowly increases with increasing exit point u up to approximately $u=-1$. From there on, $\tau(u)$ steeply grows when u approaches the origin. This confirms the qualitative picture that the motion far away from the origin is fast, while it is slow when being close to the origin $x=0$. Moreover, Fig. 5 indicates that the first fast part of the motion is almost independent of noise strength D, i.e., that the random force has little influence in this region.

V. REFLECTIONS, APPLICATIONS, AND SUMMARY

Dynamic bimodality is a general feature in monostable systems with an almost flat potential in a neighborhood of the stable state and a steep increase beyond this neighborhood. In the distribution of initial states remote regions beyond the flat neighborhood must have sufficient weight compared to the equilibrium distribution of the system. In the prior literature [16], the so-termed phenomenon of the "transient bimodality" has been studied in *asymmetric*, bistable systems. This latter phenomenon occurs above (or below) an up-switching threshold as a consequence of diffusion and the asymmetry of the potential and is closely related to the phenomenon of critical slowing down. Initially, the system starts from the point x_0 far from the stationary point, i.e., $p(x,t=0)=\delta(x-x_0)$. Next, the density $p(x,t)$ broadens and develops a long tail in the direction of the potential well giving rise to a second peak, corresponding to the stationary stable state. Our case, in contrast, refers to *symmetric* potentials and symmetric, broadened initial distributions with a probability maximum assumed at the stationary stable state.

There are various potential applications of the effect of dynamic bistability. Depending on the physical interpretation of the variable x the most probable values of magnetic fluxes, currents, or magnetization can take on nonzero values also above the critical temperature. Put differently, one can obtain transient ordered phases manifested, e.g., in short-living magnetic moments in Josephson junctions or currents in mesoscopic rings whenever the initial preparation scheme is chosen with a sufficient broadness. These ordered transient phases could be used for generating magnetic or electric impulses of a certain lifetime which can be "programmed" by a proper choice of initial conditions, or by a tuning of parameters in the system.

In summary, some interesting, rather general features of the dynamics of systems approaching the thermodynamic equilibrium Gibbs state have been studied by a numerical analysis of time-dependent solutions of the corresponding Fokker-Planck equation. For a wide class of models and a wide class of initial states, the initially and finally monostable system can exhibit bimodal transient properties during a finite time interval. We expect these phenomena to appear in systems above a second-order phase transition. However, it is also possible in systems which do not exhibit any critical behavior. This study is therefore of a relevance to a broad class of systems modeling a rich diversity of processes in nature. We hope that these transient bimodality phenomena might find their way into applications like the generation and the control of short magnetic or electric impulses. Within the bimodality regime, nonzero fluxes and currents can emerge: they survive for some time and finally die away. If the survival time is made sufficiently long, such intriguing bimodal, transient fluxes and currents can be ob-

served in such systems as Josephson junctions, mesoscopic cylinders, or magnetic bistable nanostructures like nanodots and nanorings [17].

ACKNOWLEDGMENTS

We acknowledge the financial support by the Foundation for Polish Science under Grant No. SN-302-934 (J.D.), the Ministry of Education and Science via Grant No. PBZ-MIN-008/P03/2003, Grant No. 1 P03B 071 30 (M.M.), and the ESF (Stochastic Dynamics: fundamentals and applications) (J.Ł., P.T., and P.H.).

APPENDIX

For a one dimensional Markov process $x(t)$, which is defined by the Langevin equation (1) the mean first time $\mathcal{T}_a(x_0 \to u)$ to cross the boundary point $x=u$ of the interval $[a,u]$ is intimately related to the inverse of an escape rate [1,15]. After having started out at $x_0 \in [a,u]$ it is obtained by use of a reflecting boundary set at $x=a$ and an absorbing boundary at $x=u$ in terms of a closed form expression consisting of two quadratures [see Eq. (7.8) in Ref. [1]],

$$\mathcal{T}_a(x_0 \to u) = \frac{1}{D}\int_{x_0}^{u} dy e^{V(y)/D} \int_a^y dz e^{-V(z)/D}. \tag{A1}$$

Given this expression one immediately obtains the mean time $\tau(u)$ it takes to reach the boundary u of the interval $[a,u]$ after the process has started out at the other boundary point a, namely,

$$\tau(u) \equiv \mathcal{T}_a(a \to u) = \frac{1}{D}\int_a^u dy e^{V(y)/D} \int_a^y dz e^{-V(z)/D}. \tag{A2}$$

Differentiating $\tau(u)$ twice with respect to u one finds that this *time of first exit* satisfies the inhomogeneous backward equation

$$L^+\tau(u) = 1 \tag{A3}$$

with the homogeneous "initial conditions"

$$\tau(a) = 0, \quad \tau'(a) = 0. \tag{A4}$$

Here L^+ denotes the backward operator of the considered process

$$L^+ = -V'(u)\frac{d}{du} + D\frac{d^2}{du^2}. \tag{A5}$$

Notably, this equation differs from the well known Pontryagin-Andronov-Vitt relation [1] for the mean first passage time $\mathcal{T}_a(x \to u)$ as a function of x by the sign of the inhomogeneity and the nature of the boundary conditions.

[1] P. Hänggi, P. Talkner, and M. Borkovec, Rev. Mod. Phys. **62**, 251 (1990).
[2] P. Hänggi, J. Stat. Phys. **42**, 105 (1986); **44**, 1003 (1986) (Addendum).
[3] P. Hänggi and P. Jung, Adv. Chem. Phys. **89**, 239 (1995).
[4] L. Gammaitoni, P. Hänggi, P. Jung, and F. Marchesoni, Rev. Mod. Phys. **70**, 223 (1998); P. Hänggi, ChemPhysChem **3**, 285 (2002).
[5] E. Abraham and S. D. Smith, Rep. Prog. Phys. **45**, 815 (1982).
[6] P. Talkner and P. Hänggi, Phys. Rev. A **29**, 768 (1984); C. Zerbe, P. Jung, and P. Hänggi, Z. Phys. B: Condens. Matter **86**, 151 (1992).
[7] P. Hänggi and H. Thomas, Phys. Rep. **88**, 207 (1982).
[8] H. Risken, *The Fokker-Planck Equation* (Springer, Berlin, 1984).
[9] H. E. Stanley, *Introduction to Phase Transitions and Critical Phenomena* (Oxford University Press, Oxford, 1971), cf. part III.
[10] J. K. Bhattacharjee, P. Meakin, and D. J. Scalapino, Phys. Rev. A **30**, 1026 (1984).
[11] A. Barone and G. Paternó, *Physics and Application of the Josephson Effect* (Wiley, New York, 1982).
[12] F. Hund, Ann. Phys. **32**, 102 (1938); U. Eckern and P. Schwab, J. Low Temp. Phys. **126**, 1291 (2002).
[13] L. P. Levy *et al.*, Phys. Rev. Lett. **64**, 2074 (1990); V. Chandrasekhar *et al.*, *ibid.* **67**, 3578 (1991); D. Mailly *et al.*, *ibid.* **70**, 2020 (1993); B. Reulet *et al.*, *ibid.* **75**, 124 (1995); E. M. Q. Jariwala *et al.*, *ibid.* **86**, 1594 (2001); W. Rabaud *et al.*, *ibid.* **86**, 3124 (2001); R. Deblock *et al.*, *ibid.* **89**, 206803 (2002).
[14] J. Dajka, J. Łuczka, M. Szopa, and E. Zipper, Phys. Rev. B **67**, 073305 (2003); J. Dajka, J. Łuczka, M. Szopa, and P. Hänggi, Phys. Status Solidi B **242**, 196 (2005).
[15] P. Reimann, G. J. Schmid, and P. Hänggi, Phys. Rev. E **60**, R1 (1999).
[16] F. Baras, G. Nicolis, M. Malek Mansour, and J. W. Turner, J. Stat. Phys. **32**, 1 (1983); G. Broggi and L. A. Lugiato, Phys. Rev. A **29**, 2949 (1984); G. Broggi, L. A. Lugiato, and A. Colombo, *ibid.* **32**, 2803 (1985).
[17] X. Y. Kong, Y. Ding, R. Yang, and Z. L. Wang, Science **303**, 1348 (2004); H. F. Ding *et al.*, Phys. Rev. Lett. **94**, 157202 (2005); F. Q. Zhu *et al.*, *ibid.* **96**, 027205 (2006).